

Research Article

Flavonoid derivative DMXAA attenuates cisplatin-induced acute kidney injury independent of STING signaling

Lingling Lu^{1,2,3,*}, Weihua Liu^{1,2,3,*}, Shumin Li^{1,2,3,*}, Mi Bai^{1,2,3}, Yu Zhou^{1,2,3}, Zhaohui Jiang^{1,2,3},  Zhanjun Jia^{1,2,3}, Songming Huang^{1,2,3}, Aihua Zhang^{1,2,3} and  Wei Gong^{1,2,3}

¹Nanjing Key Laboratory of Pediatrics, Children's Hospital of Nanjing Medical University, Nanjing, China; ²Jiangsu Key Laboratory of Pediatrics, Nanjing Medical University, Nanjing, China; ³Department of Nephrology, Children's Hospital of Nanjing Medical University, Nanjing, China

Correspondence: Wei Gong (gongwei@njmu.edu.cn) or Aihua Zhang (zhaihua@njmu.edu.cn) or Songming Huang (smhuang@njmu.edu.cn)

Cisplatin-induced nephrotoxicity is the main adverse effect of cisplatin-based chemotherapy and highly limits its clinical use. DMXAA, a flavonoid derivative, is a promising vascular disrupting agent and known as an agonist of STING. Although cGAS-STING activation has been demonstrated to mediate cisplatin-induced acute kidney injury (AKI), the role of DMXAA in this condition is unclear. Here, we defined an unexpected and critical role of DMXAA in improving renal function, ameliorating renal tubular injury and cell apoptosis, and suppressing inflammation in cisplatin-induced AKI. Moreover, we confirmed that DMXAA combated AKI in a STING-independent manner, as evidenced by its protective effect in STING global knockout mice subjected to cisplatin. Furthermore, we compared the role of DMXAA with another STING agonist SR717 in cisplatin-treated mice and found that DMXAA but not SR717 protected animals against AKI. To better evaluate the role of DMXAA, we performed transcriptome analyses and observed that both inflammatory and metabolic pathways were altered by DMXAA treatment. Due to the established role of metabolic disorders in AKI, which contributes to kidney injury and recovery, we also performed metabolomics using kidney tissues from cisplatin-induced AKI mice with or without DMXAA treatment. Strikingly, our results revealed that DMXAA improved the metabolic disorders in kidneys of AKI mice, especially regulated the tryptophan metabolism. Collectively, therapeutic administration of DMXAA ameliorates cisplatin-induced AKI independent of STING, suggesting a promising potential for preventing nephrotoxicity induced by cisplatin-based chemotherapy.

Introduction

Cisplatin is a chemotherapy drug that is used in cancer therapy. It is widely utilized in many kinds of solid neoplasm treatments, such as those for testicular, lung, ovarian and breast cancer [1]. However, the deleterious side effects of cisplatin limit its use in clinical practice. To date, numerous side effects of cisplatin therapy have been reported, including nephrotoxicity, gastrointestinal toxicity, ototoxicity and neurotoxicity [2]. Among these side effects, nephrotoxicity is the main dose-limiting one. Kidney is an organ that is sensitive to cisplatin because cisplatin can be transported into renal epithelial cells and accumulates within the kidney, which makes the concentrations of cisplatin in the kidney exceed those in the blood [3]. Cisplatin nephrotoxicity has several manifestations, but one of the most serious and relatively common presentations is acute kidney injury (AKI), which has an incidence of 20–30% in patients [4,5]. Clinically, the current treatment strategy is symptomatic without significant effectiveness, and there remains an unmet need for effective therapies to prevent cisplatin-induced AKI.

*These authors contributed equally to this work.

Received: 15 November 2022

Revised: 17 February 2023

Accepted: 22 February 2023

Accepted Manuscript online:

23 February 2023

Version of Record published:

21 March 2023

DMXAA (also known as vadimezan or ASA404), a flavonoid derivative, is considered one of the most promising vascular disrupting agents that displays remarkable antitumor properties [6]. Knowledge of DMXAA developed through two phases: before and after the stimulator of interferon genes (STING) was discovered [7]. Initially, studies of DMXAA focused on its antitumor activity and the underlying mechanism. After STING was identified in 2008, DMXAA was demonstrated to be a murine agonist of STING and could trigger STING–TBK1–IRF3 signaling [8–10]. Although the species differences in STING restrict the clinical use of DMXAA, its sensitivity to murine STING makes DMXAA an outstanding agonist and has been applied in STING-related studies [11,12].

Recently, Hiroshi Maekawa et al. reported that the STING pathway is a critical regulator in cisplatin-induced AKI [13]. STING knockout (KO) mice showed less kidney injury when subjected to cisplatin, and STING inhibitors significantly ameliorated tubular injury and inflammation in cisplatin-induced AKI mice [13,14]. It is postulated that DMXAA, an agonist of STING, would aggravate cisplatin-induced AKI in mice. However, our results suggested that DMXAA could ameliorate cisplatin-induced kidney injury, as demonstrated by the improved renal function, reduced tubular injury score and other mitigated tubular injury markers. Using STING global knockout mice and another STING agonist, SR717 [15], we found that DMXAA protected against cisplatin-induced AKI mainly in a STING-independent manner. Transcriptome analyses using RNA-seq data from DMXAA-treated mice combined with an available dataset in cisplatin-induced AKI indicated that inhibiting inflammation and reversing metabolic disorders might be involved in the mechanism by which DMXAA combated cisplatin-induced AKI. Further metabolomics performed on kidney tissues from cisplatin-induced AKI mice with or without DMXAA treatment revealed that DMXAA improved the metabolic disorders, especially the tryptophan metabolism in kidneys of AKI mice. Based on these findings, we report that DMXAA can ameliorate cisplatin-induced AKI in a STING-independent manner and has promising therapeutic potential for combating cisplatin nephrotoxicity.

Materials and methods

Reagents and antibodies

DMXAA (HY-10964) and SR717 (HY-131454) were purchased from MedChemExpress (Princeton, NJ, U.S.A.). Dimethyl sulfoxide (DMSO, V900090) was purchased from Sigma–Aldrich (St. Louis, MO, U.S.A.). Q-PCR Master Mix (q111-02/03) and a TUNEL staining kit (A112-01/02/03) were obtained from Vazyme (Nanjing, China). ELISA kits for mouse TNF- α (1217202) and IL-6 (1210602) were ordered from Dakewe (Beijing, China). The primary antibodies for western blots or immunofluorescence were as follows: anti-STING (19851-1-AP, Proteintech, Wuhan, China), anti-neutrophil gelatinase-associated lipocalin (NGAL, ab63929, Abcam, Cambridge, U.K.), anti-kidney injury molecule 1 (KIM-1, R&D systems, Minneapolis, MN, U.S.A.), anti-cleaved caspase-3 (9664, Cell Signaling Technology, Beverly, MA, U.S.A.), anti- β -actin (AP0060, Bioworld, Shanghai, China), and anti-F4/80 (GB11027, Servicebio, Wuhan, China). The secondary antibodies labeled with horseradish peroxidase were purchased from Beyotime (Shanghai, China), and Alexa Fluor 532-labeled goat anti-rabbit IgG was obtained from Invitrogen (A-11009, Rockford, U.S.A.).

Mice and *in vivo* studies

Wild-type mice (C57BL/6J) and global STING knockout mice (*TMEM173*^{−/−}) were purchased from GemPharmatech (Nanjing, China) and maintained under standard environmental conditions. The mice were allowed free access to water and food. All animal experiments were performed in the Animal Core Facility of Nanjing Medical University and all procedures were approved by the Nanjing Medical University Institutional Animal Care and Use Committee.

A single intraperitoneal injection of cisplatin (25 mg/kg) was used to induce AKI, as previously reported [14]. To assess the effect of DMXAA, the mice were injected intraperitoneally with DMXAA (10 mg/kg) or vehicle 1 h before cisplatin injection and continued once daily. Another STING agonist, SR717 (15 mg/kg) was administered in the same manner. The mice were killed by exsanguination under isoflurane 72 h after cisplatin injection. Blood samples and kidney tissues were collected for further analysis. Besides, for detecting the potential toxic effect of DMXAA on organs, another separate experiment was performed by treating mice with DMXAA (10 mg/kg, intraperitoneal injection) or vehicle for three consecutive days. Similarly, blood samples and kidney tissues were collected after administration.

Assessment for the functions of kidney, heart, and liver

Renal function is usually assessed by blood urea nitrogen (BUN) and serum creatinine (Scr) levels. Meanwhile, we detected the serum levels of lactate dehydrogenase (LDH) and creatine kinase-MB (CK-MB) to evaluate the cardiac injury, and the level of aspartate aminotransferase (AST) to evaluate the liver function. Briefly, serum samples were

obtained from the full blood samples through centrifugation at 4000 rpm for 15 min. A serum biochemical autoanalyzer (Hitachi 7600, Tokyo, Japan) at the biochemistry laboratory of Nanjing Children's Hospital was used to measure the concentrations of BUN, Scr, LDH, CK-MB, and AST in each serum sample.

Histological analyses

For histological analysis, kidney tissues were fixed in 4% formaldehyde solution overnight and then dehydrated and embedded into paraffin blocks. Sections with a thickness of 3 μ m were stained with hematoxylin and eosin (H&E). The levels of tissue damage and inflammation were scored as previously described [16].

Immunofluorescence

The mice kidney tissues were fixed in 4% paraformaldehyde overnight for subsequent paraffin embedding and then sectioned into 3 μ m using a Leica microtome (Leica Microsystems, Buffalo Grove, Germany). After deparaffinization, rehydration, and antigen retrieval by heating in citrate buffer (pH 6.0), the sections were blocked with normal serum, and then were incubated with rabbit polyclonal antibody against F4/80 overnight at 4°C. The sections were washed with PBS and incubated with anti-rabbit Alexa Fluor 532 (1:500) secondary antibody for 1 h. Finally, the sections were washed with PBS and mounted with mounting medium with DAPI (Zhong Shan Golden Bridge, Beijing, China). Images were acquired with confocal microscopy (LSM 710, Carl Zeiss, Germany) and the number of F4/80-positive cells in each kidney section was counted.

Western blotting analysis

The western blot assay was carried out according to a previously reported method [17]. Briefly, kidney tissues were lysed in RIPA buffer (P0045, Beyotime, Shanghai, China) containing protease inhibitors (04693132001, Roche, Laval, Canada). After extraction, the concentration of protein solution was measured by a bicinchoninic acid (BCA) protein assay kit (P0012, Beyotime). About 50 μ g protein samples were mixed with loading dye, boiled and then separated by SDS-PAGE gel, and then transferred on to PVDF membranes at 300 mA for 60 min. After blocking with 5% non-fat milk, the membranes were incubated with specific antibodies against the proteins of interest at 4°C overnight and then with the secondary antibodies for 2 h at room temperature. The images of the blots were recorded by the ChemiDoc XRS+ imaging system (Bio-Rad) and analyzed using ImageJ software. β -Actin was used as the internal reference.

Apoptosis assay via TUNEL staining

Tubular cell apoptosis was detected by TUNEL staining according to the manufacturer's instructions. For details, the renal paraffin sections were deparaffinized and rehydrated and then incubated with proteinase K. After washing with PBS, the sections were cultured with TUNEL reaction solution. Images were displayed by laser scanning confocal microscopy (Carl Zeiss) and the number of TUNEL-positive apoptotic cells was counted.

Cytokine assays using ELISA

The concentrations of TNF- α and IL-6 in the mouse serum were measured by ELISA kits following the manufacturer's instructions. The absorbance of each sample was analyzed by Synergy-H1 fluorimeter from Bio-Tek (Winooski, VT, U.S.A.).

RNA-seq

C57BL/6J mice were treated with DMXAA (10 mg/kg) or vehicle through intraperitoneal injection daily for 3 days. After administration, kidney tissues were harvested, from which the total RNA was isolated using Trizol reagent. Illumina TruSeq RNA Sample Prep Kit (FC-122-1001) was used with 0.4 μ g of total RNA for the construction of sequencing libraries and HISAT2 was used to align the clean reads to the reference genome. The expression of each gene was calculated with the featureCounts tool in subread.

Bioinformatics analysis

Differential expression analysis was performed using the DESeq2 R package (1.16.1). DESeq2 provides statistical routines for determining differential expression in digital gene expression data using a model based on the negative binomial distribution. The resulting *P*-values were adjusted using Benjamini and Hochberg's approach for controlling the false discovery rate (FDR). Genes with an adjusted *P*-value <0.05 found by DESeq2 were considered differentially expressed genes (DEGs).

In addition, the RNA-seq datasets GSE153625, which were performed on the kidney tissues from control ($n=8$) and cisplatin-treated mice ($n=4$), were downloaded from the Gene Expression Omnibus (GEO) database (GSE153625, [18]). DESeq2 was used to identify the DEGs with an FDR P -value <0.05 and a \log_2 (FC) ≥ 1.5 . The DEGs in the DMXAA-treated profile and the cisplatin-treated profile were subjected to Venn diagram analysis to identify the overlapping genes between cisplatin-induced/decreased DEGs and DMXAA-decreased/induced DEGs, respectively. Then, the overlapping genes were subjected to biochemical pathway analysis using Kyoto Encyclopedia of Genes and Genomes (KEGG) and visualized in R software.

Quantitative real-time PCR analysis

Total RNA from kidney tissues was extracted and reverse transcribed for quantitative real-time PCR (qRT-PCR). qRT-PCR was performed to detect the target gene expression in kidney tissues of mice [19]. Relative amounts of mRNA were calculated using delta delta Ct method as normalized to the 18S control. The sequences of the primers were as follows: CXCL1, forward 5'-TAGGGTGAGGACATGTGTGG-3' and reverse 5'-AAATGTCCAAGGGAAGCGT-3'; CXCL2, forward 5'-TGCCAAGGGTTGACTTCAAGA-3' and reverse 5'-ACTTTTGGACCGCCCTTGAGA-3'; TNF- α , forward 5'-TGATCGGTCCCCAAAGGGAT-3' and reverse 5'-TTTGCTACGACGTGGGCTAC-3'; IL-6, forward 5'-TAGTCCTTCTACCCCAATTTCC-3' and reverse 5'-TTGGTCCTTAGCCACTCCTTC-3'; COX2, forward 5'-AGGACTCTGCTCAGGAAGGA-3' and reverse 5'-TGACATGGATTGGAACAGCA-3'; 18S, forward 5'-TTCGGAAGTGAAGGCCATGATT-3' and reverse 5'-TTTCGCTCTGGTCCGTCTTG-3'.

Untargeted metabolomics analysis

About 30 mg of kidney tissues was homogenized in 400 μ l ice-cold extracting solution and then centrifuged at 12000 rpm for 15 min. Equal amounts of samples were concentrated and dried *bi vacuum*, then dissolved in 50% methanol. After ultrasonic treatment and centrifugation, the supernatant was used for the following metabolomics study.

Samples were put at the auto-sampler whose temperature was set at 4. Chromatographic separation was carried out using an ACQUITY UPLC[®] HSS T3 (Waters, 1.7 μ m, 150 \times 2.1 mm) column maintained at 40°C and the injection volume was 2 μ l. Mobile phase A and B were 0.1% formic acid in water and in methanol, respectively. The gradient conditions were as follows: positive model: 0–0.5 min, B/D: 2%; 0.5–6 min, B/D: 2–50%; 6–10 min, B/D: 50–98%; 10–14 min, B/D: 98%; 14–16 min, B/D: 98–2%; 16–21 min, B/D: 2%. Metabolites were assayed separately in positive and negative electrospray ionization (ESI) models. Five quality control (QC) samples from mixed samples were run throughout the analytical process to assure stability and reliability of the assays.

Metabolites identification was carried out using Compound Discovery software. The *ropls* R package implements multivariate analysis including the PCA, PLS-DA and OPLS-DA. Significantly altered metabolites were identified based on a Student's t -test with a P -value <0.05 and $|\text{FC (fold change)}| > 2$, then labeled with KEGG ID using Thermo Scientific[™] Compound Discoverer[™] 3.1 software for further metabolic pathway enrichment analysis in KEGG databases.

Statistical analysis

GraphPad Prism 7 was used to perform statistical tests and to generate graphs. Data are expressed as the mean \pm SEM. Statistical analysis was performed using Student's t test or one-way ANOVA followed by Bonferroni's comparison test. P -values of <0.05 were considered significant.

Results

Treatment with DMXAA ameliorated cisplatin-induced AKI

C57BL/6J mice were treated with DMXAA or vehicle for 1 h and then administered cisplatin for another 72 h (DMXAA treatment was continued once daily, Figure 1A). Serum biochemical measurement showed that Scr and BUN levels were both decreased after DMXAA treatment, indicating an improvement in renal function (Figure 1B). Cisplatin-induced AKI is pathologically manifested by renal tubular lesions [4]; thus, we evaluated the pathologic manifestations in the mouse model. Our results of H&E staining displayed a significantly profound tubular injury, including tubular dilatation, cast formation, loss of brush border and tubular epithelial damage induced by cisplatin; however, these pathological changes were ameliorated by DMXAA treatment (Figure 1C,D). Consistently, the kidney injury markers KIM-1 and NGAL were also dramatically decreased after DMXAA administration (Figure 1E,F). Of note, the current dose of DMXAA used in mice experiments had no significant toxic effect on kidney morphology or the functions of kidney, heart, and liver (Figure 2A–D).

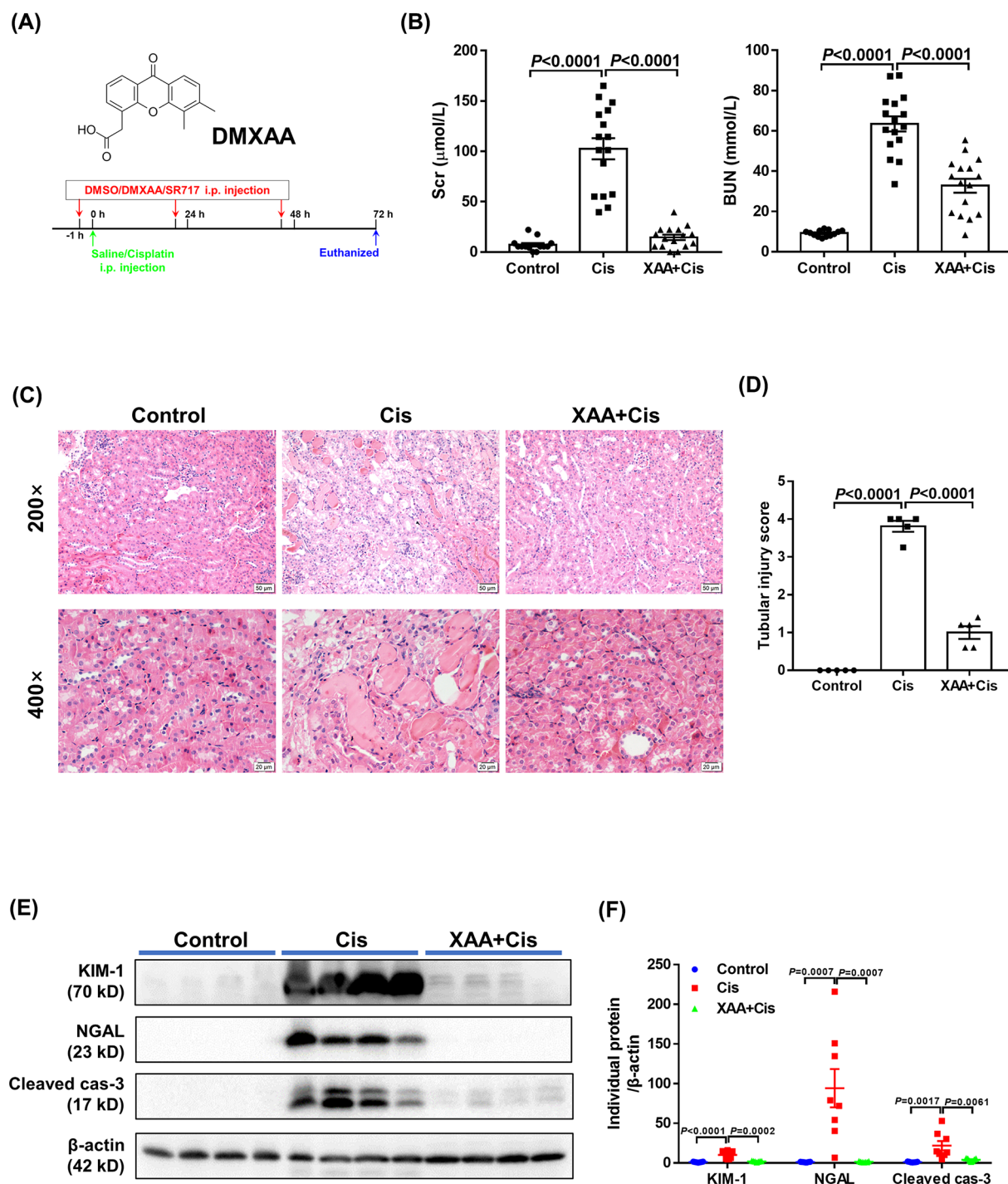


Figure 1. DMXAA treatment ameliorated renal dysfunction and tubular injury induced by cisplatin

(A) The chemical structure of DMXAA and the schematic representation of the experimental design for administration with DMXAA or SR717 in a mouse model of cisplatin-induced AKI. (B) Serum levels of creatinine (Scr) and blood urea nitrogen (BUN) were assessed, $n=13$ –16 per group. (C) Representative images of H&E-stained kidney sections. (D) Analysis of tubular injury score, $n=5$ per group. (E) Representative Western blot images for KIM-1, NGAL, and cleaved cas-3. (F) Densitometry analysis of the Western blots ($n=7$ –8 per group). Data are expressed as the mean \pm SEM, and each significant P -value is labeled in the indicated place.

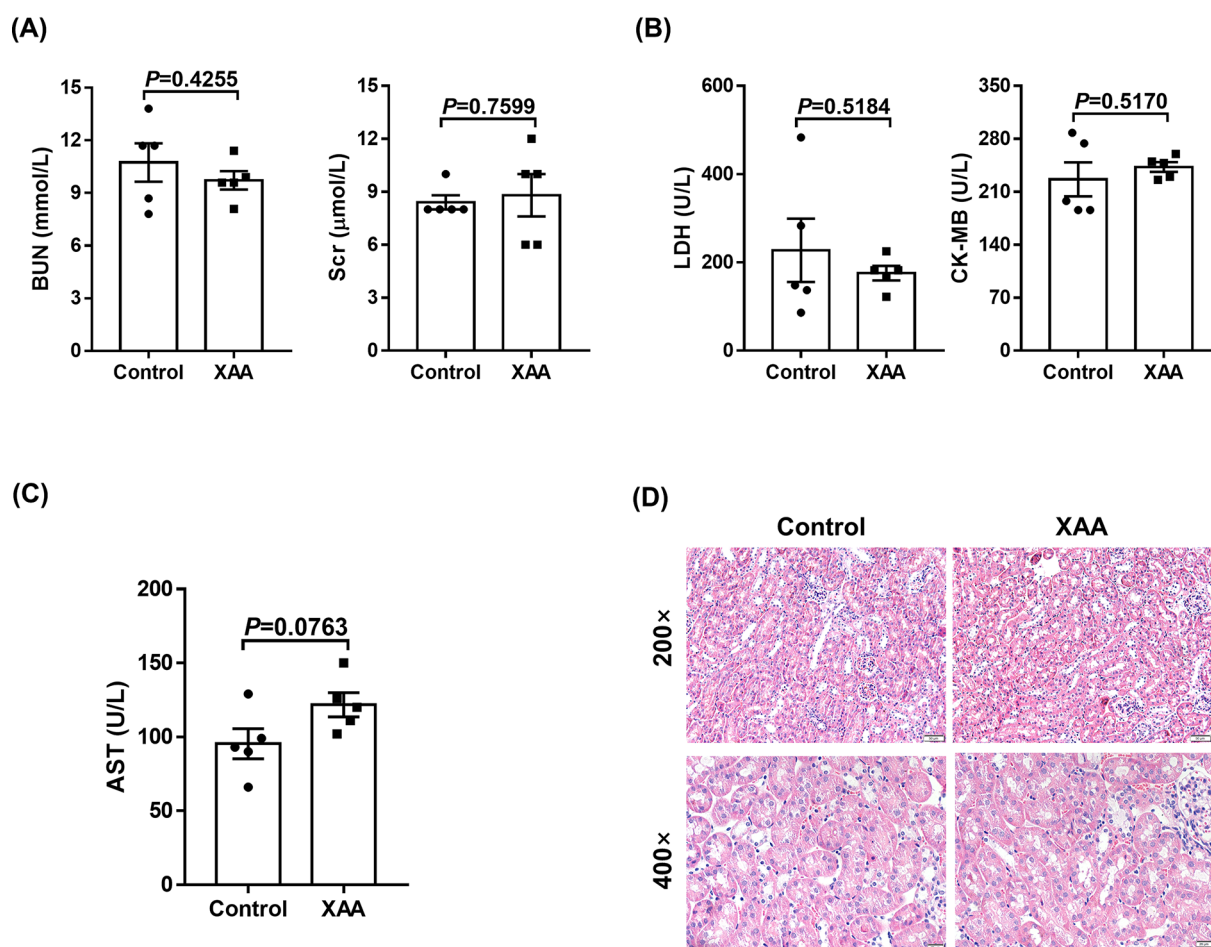


Figure 2. Assessment for the toxicity of DMXAA in mice

C57BL/6J mice were administered with DMXAA or vehicle for three consecutive days and serum levels of BUN and Scr (A), LDH and CK-MB (B) and AST (C) were measured, $n = 5$ per group. Data are expressed as the mean \pm SEM, and each P -value is labeled in the indicated place. (D) Representative images of H&E-stained kidney sections from mice receiving injection of DMXAA or vehicle.

DMXAA inhibited renal tubular cell apoptosis and inflammation in cisplatin-induced AKI mice

Next, we used TUNEL staining and Western blotting analysis to compare tubular cell apoptosis after DMXAA administration. We found that renal tubular cell apoptosis was attenuated, as evidenced by the decreased TUNEL-positive cell counts (Figure 3A,B) and cleaved caspase-3 expression (Figure 1E,F). Besides, F4/80 staining to detect macrophages in the kidneys revealed a prominent infiltration after cisplatin treatment, while DMXAA-treated mice showed lower macrophage numbers (Figure 3C,D). In addition, we examined the serum levels of TNF- α and IL-6, which are the main upregulated inflammatory factors in cisplatin nephrotoxicity. Figure 3E,F showed that DMXAA reduced the serum levels of TNF- α and IL-6, indicating a significant relief of systemic inflammation. Overall, these results indicated that DMXAA protected against cisplatin-induced AKI by preserving renal tubular function, preventing cell apoptosis and reducing inflammation.

The renoprotective effect of DMXAA in cisplatin-induced AKI is not dependent on STING

Recently, DMXAA is well known as a selective activator of murine STING that has been shown to induce the activation of STING-related pathways [11,12]. In our mouse model, cisplatin induced STING expression in kidney tissues (Figure 4A,B), which is consistent with the previous study [13,14]. However, the expression of STING was significantly reduced by DMXAA treatment in the presence of cisplatin (Figure 4A,B). To determine whether DMXAA

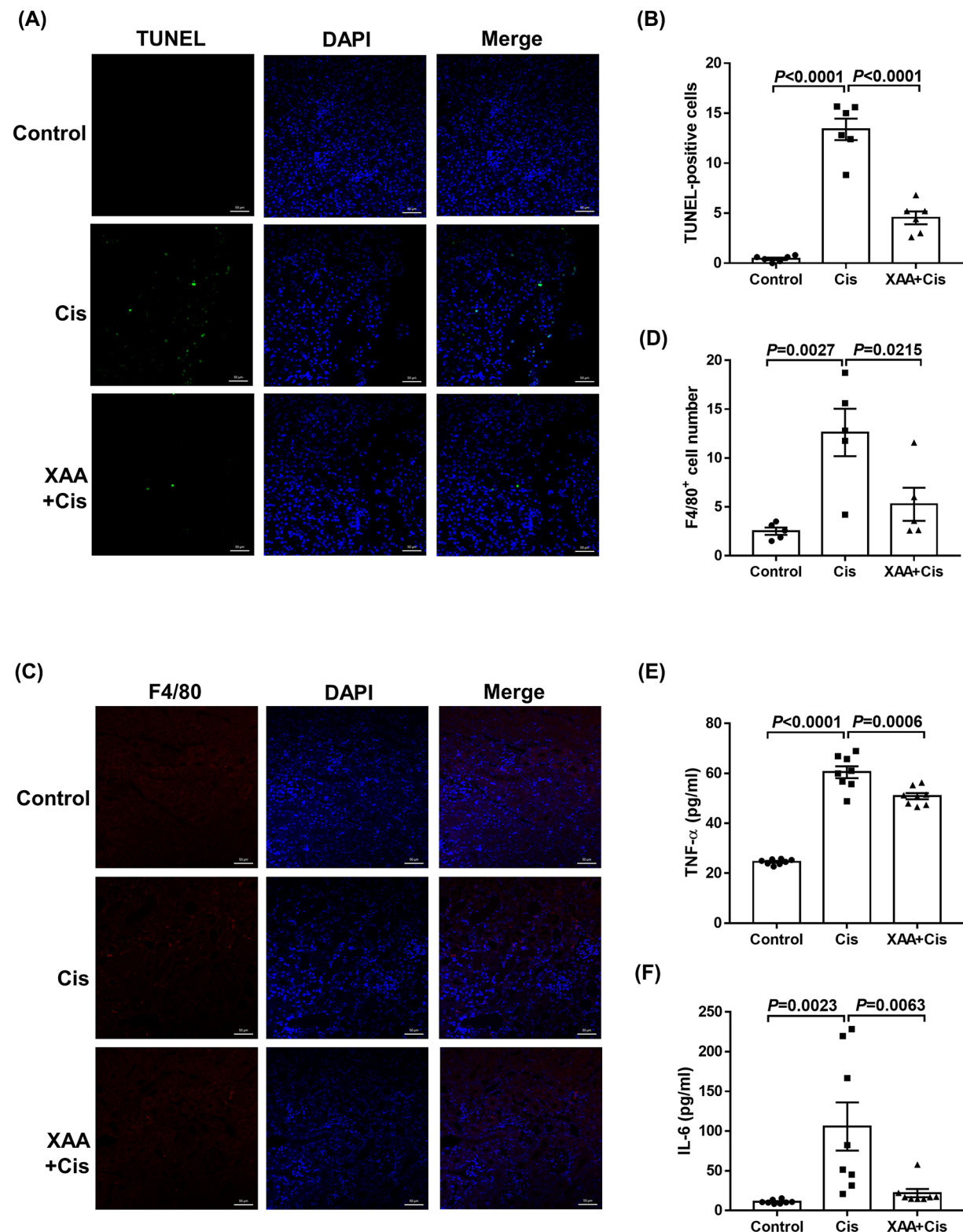


Figure 3. DMXAA treatment ameliorated renal tubular cell apoptosis and inflammation induced by cisplatin

(A) Representative images of TUNEL staining of kidney sections. (B) The column shows the TUNEL-positive cell counts, $n = 6$ per group. (C) Representative images of F4/80 staining of kidney sections. (D) The number of F4/80 positive cells in each field was counted, $n = 5$ per group. (E,F) Serum levels of TNF- α and IL-6, $n = 8$ per group. Data are expressed as the mean \pm SEM, and each significant P -value is labeled in the indicated place.

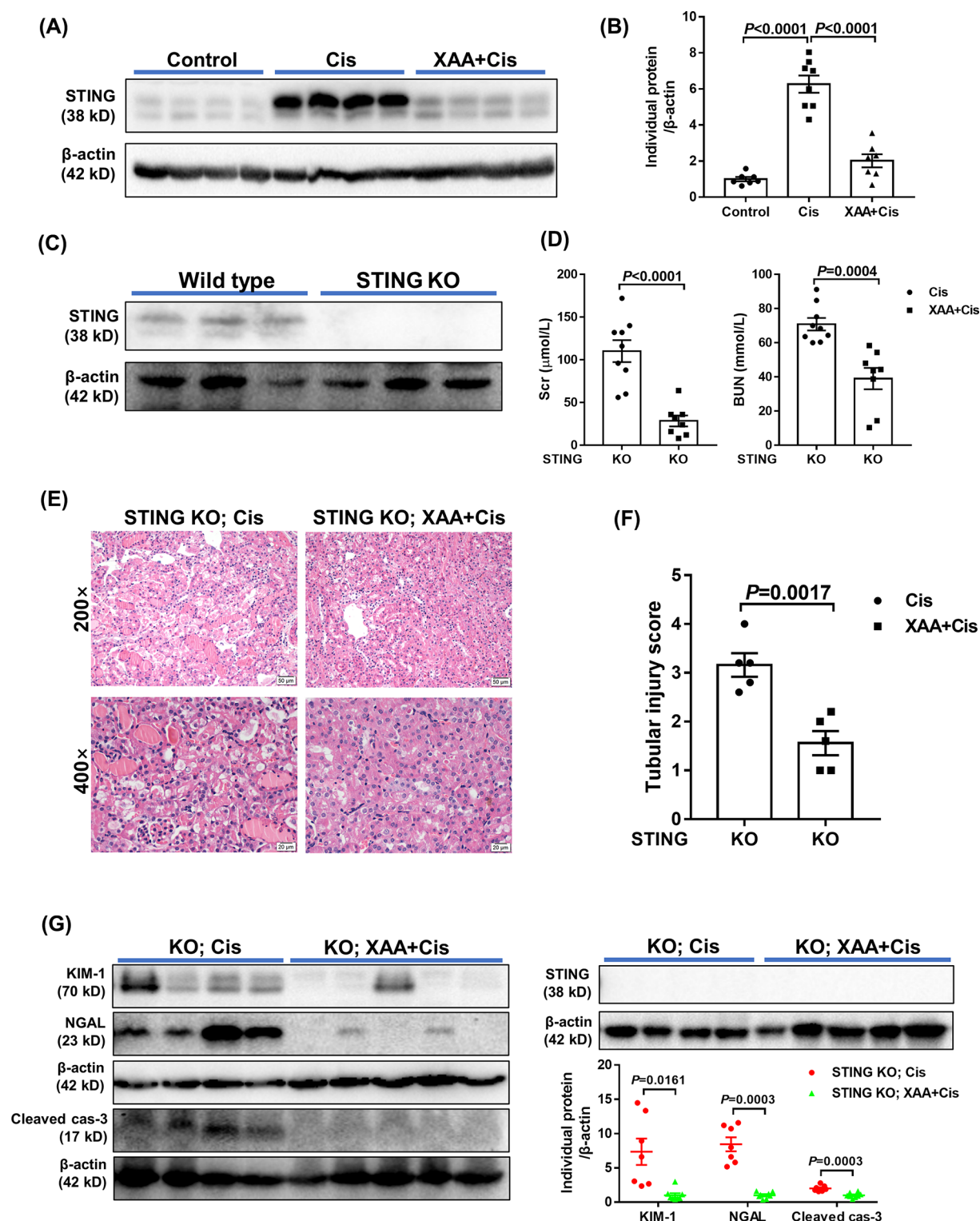


Figure 4. The protective effect of DMXAA in cisplatin-induced AKI also showed in STING KO mice

(A) Representative Western blot images for STING. (B) Densitometry analysis of the Western blots of STING ($n = 7$ –8 per group). (C) Representative Western blot images for STING protein isolated from the kidneys of wild-type and STING knockout (KO) mice, respectively. (D) Serum levels of Scr and BUN were assessed, $n = 8$ –9 per group. (E) Representative images of H&E staining are shown. (F) Analysis of tubular injury score, $n = 5$ per group. (G) Representative Western blot images for KIM-1, NGAL, cleaved cas-3, and STING. Scatter plot graph showed the densitometry analysis of the Western blots ($n = 7$ –8 per group). Data are expressed as the mean \pm SEM, and each significant P -value is labeled in the indicated place.

exerts its protective effect through STING signal pathway in cisplatin-treated mice, we utilized global STING knock-out (STING KO) mice. First, the knockout efficiency of STING was demonstrated by Western blot and there was no STING expression in STING knockout mice (Figure 4C). The STING knockout mice were divided into two groups, and were administered cisplatin with or without DMXAA treatment. The serum levels of Scr and BUN were decreased after DMXAA treatment (Figure 4D), together with the down-regulated tubular injury score (Figure 4E,F) and the expression of KIM-1, NGAL, and cleaved caspase-3 (Figure 4G). Of course, the expression of STING was not detected at this condition (Figure 4G). The existing therapeutic effects of DMXAA in STING knockout mice suggested that STING is not required for AKI amelioration by DMXAA.

To confirm this point, we used another STING agonist, SR717, in cisplatin-induced AKI mice. As shown in Figure 5, SR717 did not alleviate cisplatin-induced kidney injury, as the serum levels of Scr and BUN (Figure 5A), the pathologic damage in renal tubules (Figure 5B,C), most of kidney injury markers and STING expression (Figure 5D,E) were not altered after SR717 treatment, whereas these indicators were improved in the DMXAA-treated group (Figure 5, **XAA+Cis group**). These results indicated that DMXAA protected against cisplatin-induced AKI through STING-independent manner.

Renal transcriptome analysis in DMXAA-treated mice

To explore the molecular mechanism, whole transcriptome RNA-seq was performed in kidney samples from mice with or without DMXAA treatment (2–3 biological replicates). The volcano plot (Figure 6A) showed all 25,589 detected genes, of which 605 up-regulated genes and 388 down-regulated genes were identified with an FDR-corrected *P*-value <0.05. The top 10 up-regulated and down-regulated genes are displayed in Figure 6B. Among the most down-regulated genes, aryl hydrocarbon receptor repressor (AHRR, a repressor of AHR) has been reported to be involved in kidney disease. Particularly, inhibiting AHRR protected against cisplatin-induced AKI [20]. Meanwhile, among the most up-regulated genes, serum amyloid A protein (SAA) and matrix metalloproteinase-7 (MMP7) have been demonstrated to promote renal recovery and tubule regeneration after acute renal failure and ameliorate AKI [21,22].

To further determine the pathways involved in the protective effect of DMXAA against AKI, a published gene expression profile representing the cisplatin nephrotoxicity mouse model in the GEO database was analyzed. Eight kidney samples of sham control mice and three kidney samples of mice with cisplatin treatment were extracted from this profile (GSE153625). Following data preprocessing, 3041 DEGs were detected, among which 1700 genes were up-regulated and 1341 genes were down-regulated in the cisplatin-treated group (relative to the sham control group). Then, Venn diagram analysis was performed between cisplatin-regulated DEGs and DMXAA-regulated DEGs. The Venn diagram in Figure 6C showed that 77 DEGs were overlapped between up-regulated DEGs by cisplatin and down-regulated DEGs by DMXAA. KEGG enrichment analysis of these overlapped DEGs was then performed to identify the potentially relevant pathways involved in the protective role of DMXAA. As shown in Figure 6D, the top two pathways that were significantly enriched were the IL-17 and TNF signaling pathways, which have been reported to aggravate the development of AKI [23,24]. DEGs enriched in the IL-17 signaling pathways were positively regulated by cisplatin while negatively regulated by DMXAA, indicating a transcriptional-regulated effect of DMXAA in anti-inflammation. In accordance with this speculation, we determined the relative inflammatory factors in IL-17 signaling pathway in kidney tissues from cisplatin-challenged mice with or without DMXAA treatment. As shown in Figure 6E, CXCL1, CXCL2, IL-6, and COX2 were significantly induced by cisplatin while decreased upon DMXAA treatment. In addition, although TNF- α did not reach a statistically significant difference between cisplatin versus DMXAA+cisplatin group, it still showed a same pattern. Besides, 151 DEGs were overlapped between down-regulated DEGs by cisplatin and up-regulated DEGs by DMXAA (Figure 7A), and enrichment of these overlapping DEGs was displayed to be related to multiple metabolic pathways (Figure 7B), suggesting that DMXAA might regulate metabolism in AKI.

Furthermore, to find more potential regulated pathways by DMXAA, we performed the Venn diagram analysis again between down-regulated DEGs by cisplatin and the total DMXAA-regulated DEGs, and between down-regulated DEGs by DMXAA and the total cisplatin-regulated DEGs as well (Figure 8A,C). KEGG enrichment analysis was then performed based on the respective overlapped DEGs (shown in Figure 8A,C). We found that metabolism, IL-17 and TNF signaling pathways were also significantly enriched based on this analysis pattern (Figure 8B,D), which suggested again that the regulated metabolism and inflammatory pathways might be involved in the protective mechanism of DMXAA combating AKI.

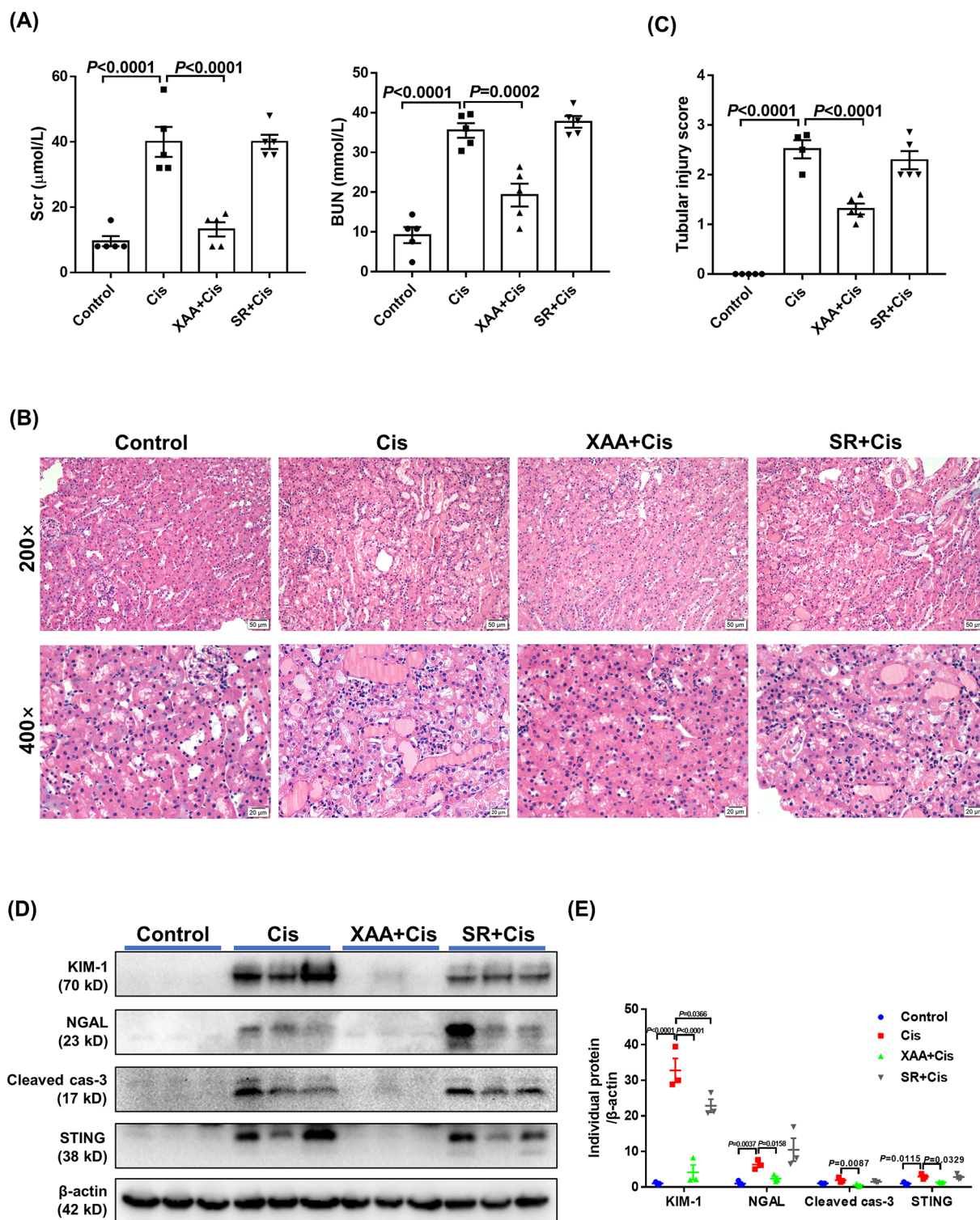


Figure 5. Another STING agonist, SR717, did not affect cisplatin-induced kidney injury

C57BL/6J mice were administered DMXAA or SR717 as described before and then challenged with cisplatin. Seventy-two hours after cisplatin injection, the mice were euthanized and the kidneys were harvested. (A) Serum levels of Scr and BUN were assessed, $n = 5$ per group. (B) Representative images of H&E staining are shown. (C) Analysis of tubular injury score, $n = 4$ –5 per group. (D) Representative Western blot images for KIM-1, NGAL, cleaved cas-3, and STING. (E) Densitometry analysis of the Western blots ($n = 3$ per group). Data are expressed as the mean \pm SEM, and each significant P -value is labeled in the indicated place.

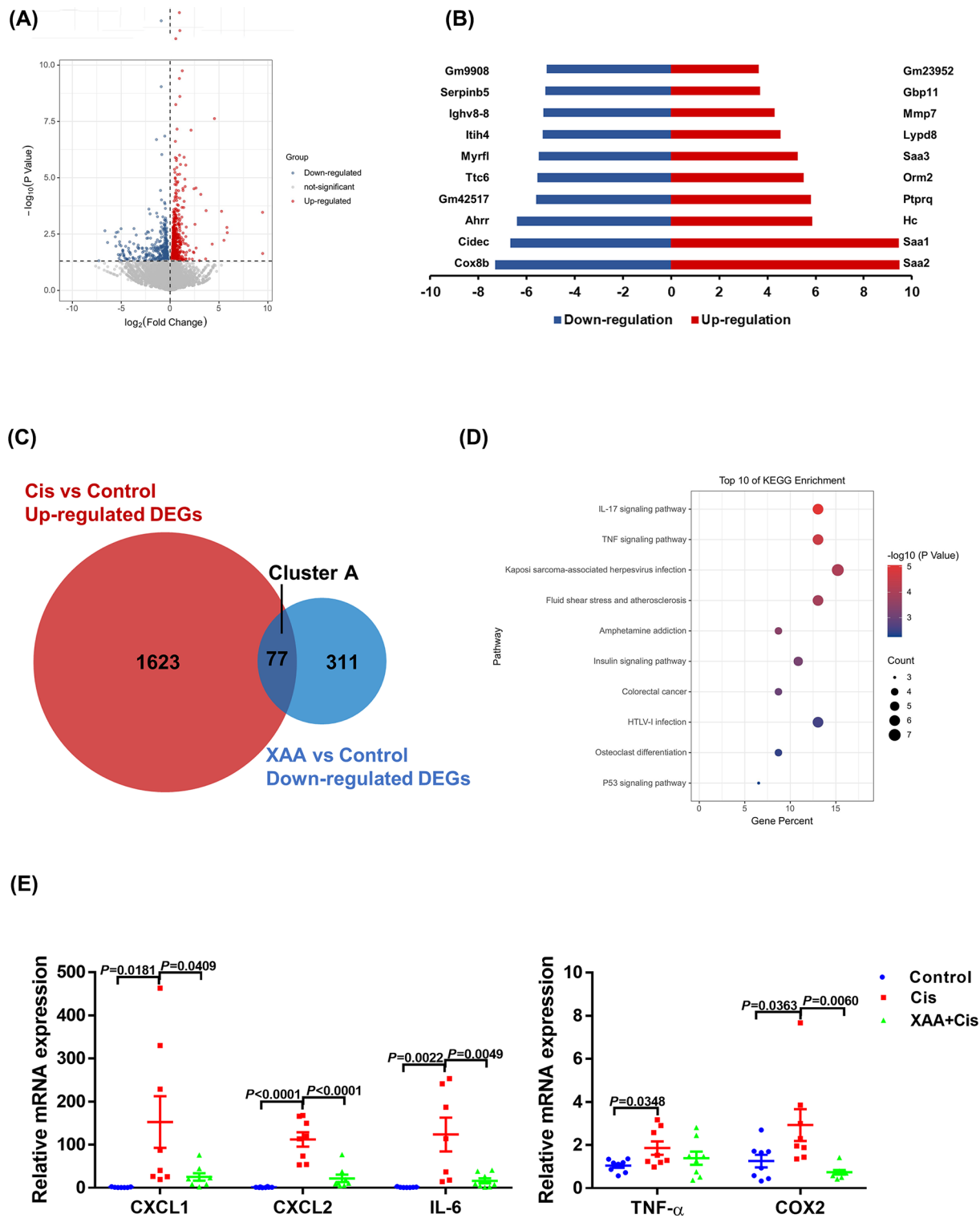


Figure 6. Renal transcriptome analysis

(A) Volcano plots showing genes whose expression was significantly regulated by DMXAA treatment. (B) Graphical depiction of the top up- and downregulated genes in the DMXAA-treated model. (C) Venn diagram depicting common differentially expressed genes (DEGs) in DMXAA-treated model and cisplatin-treated model. (D) KEGG pathway enrichment analysis of Cluster A (shown in panel C). (E) Relative expressions of inflammatory factors involved in IL-17 signaling pathway in kidney tissues from cisplatin-induced mice with or without DMXAA treatment ($n = 7-8$ per group). Data are expressed as the mean \pm SEM, and each significant P -value is labeled in the indicated place.

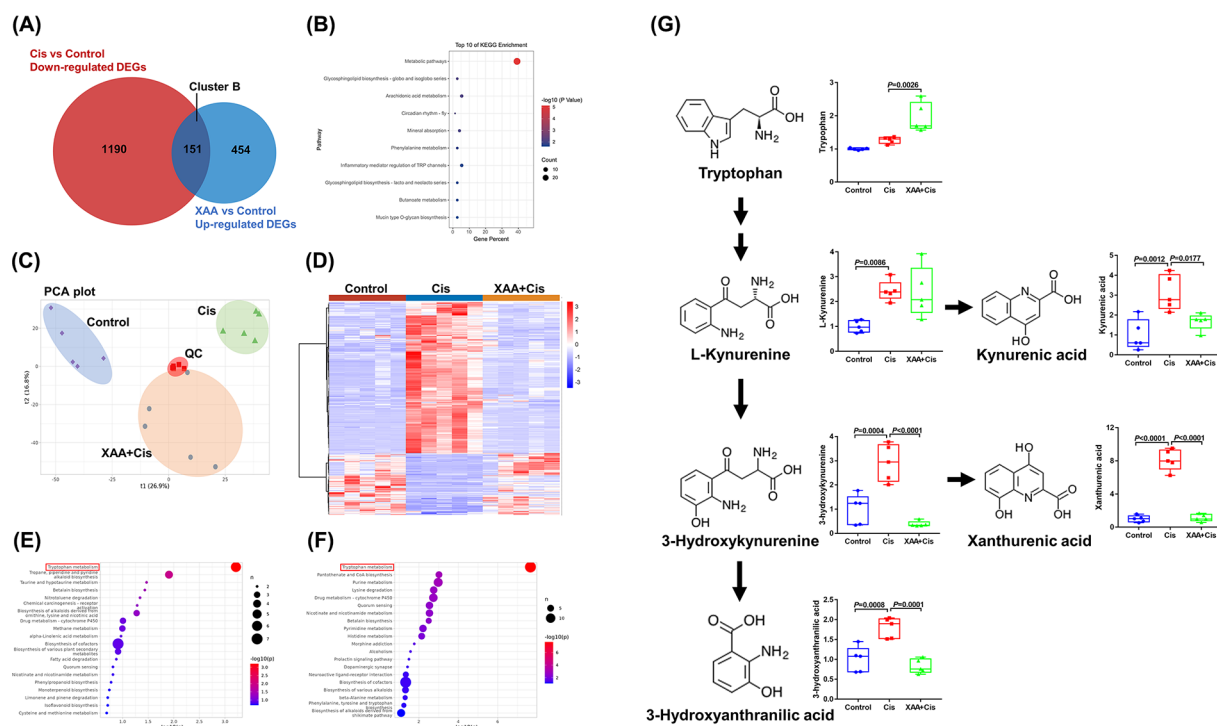


Figure 7. DMXAA restored the metabolic disturbance in cisplatin-challenged kidney tissues

(A) Venn diagram depicting common differentially expressed genes in the two RNA-seq profiles mentioned above. (B) KEGG pathway enrichment analysis of Cluster B (shown in panel A). (C–G) Metabolic profiles of AKI kidneys after DMXAA treatment were performed via LC-MS/MS. (C) The scatter plots of PCA model; QC, quality control. (D) Heat maps of averaged metabolite concentrations in kidneys of different groups. (E,F) Metabolite pathway enrichment analysis of significantly disturbed metabolites in cisplatin versus control groups (E) as well as DMXAA+cisplatin versus cisplatin groups (F). (G) Changed levels of metabolites involved in kynurenine pathway-mediated tryptophan metabolism ($n = 5$ per group). Data are expressed as the mean \pm SEM, and each significant P -value is labeled in the indicated place.

DMXAA restored metabolic disorder in kidneys from cisplatin-induced AKI mice

To confirm whether DMXAA affected metabolism during AKI, a non-targeted metabolomic analysis of kidney tissues from cisplatin-induced mice with or without DMXAA treatment was performed. The principal component analysis (PCA) score plots showed that the three groups had good reproducibility and separation (Figure 7C). Significantly altered metabolites between cisplatin versus control groups and DMXAA+cisplatin versus cisplatin groups were identified (P -value < 0.05 and $|FC$ (fold change) > 2) and shown in the heatmap (Figure 7D). Many metabolites of kidney samples from cisplatin group were significantly changed compared with control, indicating a metabolic disorder in kidney during AKI. However, these metabolites were largely normalized in DMXAA-treated group, which suggested that DMXAA could partially reverse the disturbed metabolism in AKI.

Thereafter, KEGG analysis was performed based on the significantly changed metabolites and displayed in Figure 7E,F. The most significantly altered pathways in both cisplatin versus control groups and DMXAA+cisplatin versus cisplatin groups were tryptophan metabolism. Tryptophan is an essential amino acid, which is obtained only by the food intake. Tryptophan and its metabolites are associated with numerous physiological functions. Over 95% tryptophan is catabolized through kynurenine pathway (KP) [25,26]. Previous studies suggested that tryptophan catabolism by KP was remarkably disturbed during diverse kinds of AKI, and its catabolic metabolites, such as kynurenine, 5-hydroxyindoleacetic acid and kynurenic acid were significantly elevated in urine, plasma, or kidney tissues [27–29]. In accordance with literatures, KP-catalyzed main metabolites, including L-kynurenine, kynurenic acid, 3-hydroxykynurenine, xanthurenic acid, and 3-hydroxyanthranilic acid were significantly elevated in cisplatin group while decreased by DMXAA treatment. Accordingly, the level of tryptophan was upregulated by DMXAA

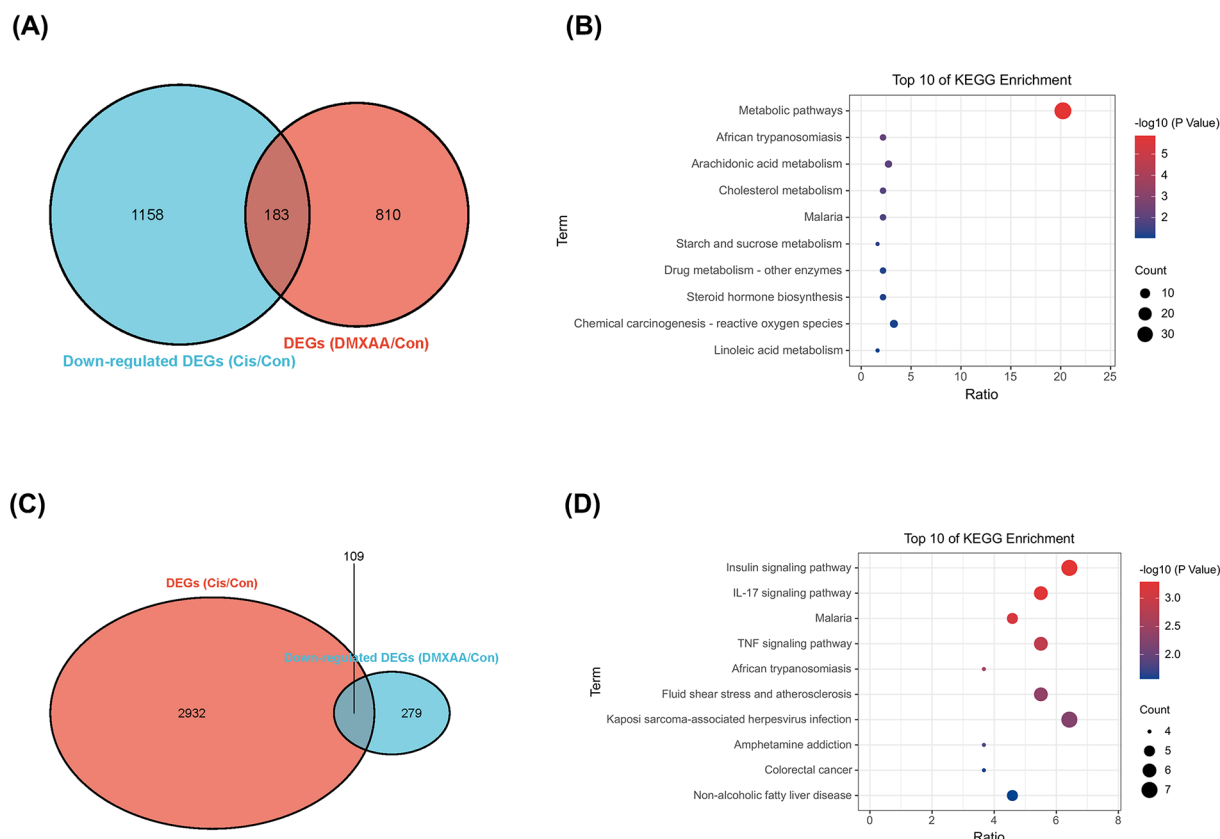


Figure 8. Extended analysis of Venn diagram and KEGG pathway enrichment based on the renal transcriptome

(A) Venn diagram analysis was performed between down-regulated DEGs by cisplatin and the total DMXAA-regulated DEGs, and the common DEGs (183) were then enriched by KEGG pathway (B). (C) Venn diagram analysis was performed between the total cisplatin-regulated DEGs and down-regulated DEGs by DMXAA, and the common DEGs (109) were then enriched by KEGG pathway (D).

treatment (Figure 7G). These data suggested that DMXAA could restore tryptophan metabolism and maintain the level of tryptophan in kidney during AKI.

Discussion

DMXAA is a promising vascular-disrupting agent that can cause irreversible destruction of tumor vessels and completely halt tumor blood flow [30]. Interestingly, DMXAA can specifically induce the shutdown of blood flow in tumors without destroying normal tissues, and for this reason, DMXAA has been widely investigated in cancer therapeutic studies and has obtained remarkable results not only in the laboratory but also in phase I/II clinical trials [7]. Studies have indicated that DMXAA can induce cell apoptosis or necrosis, the activation of the innate immune system and the production of inflammatory cytokines and nitric oxide [31–33]. Additionally, it can affect tumor energy homeostasis [34]. The exact mechanism underlying the antitumor effect of DMXAA, however, is still unknown. The discovery of STING provided theoretical evidence for the excellent antitumor activity of DMXAA. DMXAA can serve as an agonist of STING and trigger the activation of STING signaling pathways, which then promote the antitumor immune response [7,33]. Researchers have also found that DMXAA failed in phase III clinical trials because it binds only to murine STING but not human STING [11]. Nevertheless, based on this theoretical evidence, it was speculated that DMXAA aggravates AKI because STING deficiency or inhibitor attenuates cisplatin-induced tubular injury and renal dysfunction [13,14]. In fact, DMXAA has been demonstrated to induce sterile shock and aggravate cecal ligation perforation-induced abdominal sepsis without showing its effect on the related kidney injury [35]. Our findings unexpectedly demonstrated that DMXAA exerts a renoprotective effect in AKI, as evidenced by the improved renal function, reduced tubular injury score and other mitigated tubular injury markers in cisplatin-induced AKI, and this effect even occurred in STING-deficient mice. Of note, in our study, STING depletion seems to be unable to protect

against cisplatin-induced AKI, which was different from the report by Maekawa et al. [13]. Such a discrepancy could be due to the differences in the approach of gene manipulation and/or the strain origin. There are some other examples that the same gene knockout generated from different groups displayed different phenotypes in the same disease model [36,37].

To explore the underlying mechanism, we prepared RNA samples from kidney tissues of control and DMXAA-treated mice without cisplatin challenge, and then performed a transcriptomic analysis together with a published profile in the GEO database that represented a cisplatin nephrotoxicity mouse model [18]. Among the top DEGs in DMXAA (relative to the normal control), several AKI-related genes were altered for the better, including the down-regulated AHRR and the up-regulated SAA and MMP7. Moreover, the overlapping DEGs between the DMXAA-treated model and cisplatin-treated model were mainly enriched in inflammatory factor signaling pathways and some metabolic pathways. In detail, the IL-17 and TNF signaling pathways that were up-regulated in the cisplatin model were down-regulated in DMXAA-treated model, suggesting that DMXAA treatment might induce an anti-inflammatory effect in the kidney. Correspondingly, we tested the effect of DMXAA in cisplatin-treated kidney tissues and found that DMXAA significantly inhibited several inflammatory factors induced by cisplatin. However, previous reports showed that DMXAA could promote the production of inflammatory cytokines [38]. These findings indicated that the anti-inflammatory effect of DMXAA might occur through comprehensive action *in vivo*.

Furthermore, the metabolic pathways that were inhibited in cisplatin-treated model were up-regulated in DMXAA-treated model. Previous studies demonstrated that metabolic profiles changed during AKI and that these metabolic disorders may mediate potential injury in the kidney [39–42]. To further explore the effect of DMXAA on metabolism during AKI, we analyzed the changes of metabolic profiles in kidney tissues of cisplatin-induced AKI mice with or without DMXAA treatment by metabolomics assay. Our results showed that the altered metabolites in cisplatin group were largely normalized after DMXAA treatment, indicating a regulatory effect of DMXAA on maintaining metabolism homeostasis during AKI. KEGG analysis showed that the pathways being most regulated by DMXAA was tryptophan metabolism. The level of tryptophan in the body is maintained not only by the food intake but the catabolic pathways [43]. Kynurenate pathway (KP)-mediated tryptophan metabolism is involved in pathological processes including inflammation, cancer, neuronal, and intestinal diseases [26,44]. Although most of the metabolites in kynurenine pathway have not been studied in AKI, previous studies including clinical data have demonstrated that the abnormality of KP-mediated tryptophan metabolism was closely related to AKI and has been suggested as a promising target in the diagnosis and prognosis of AKI [27–29,45–48]. For example, in the urine from AKI patients with cardiac surgery under cardiopulmonary bypass, the ratios of kynurenine metabolites to tryptophan were highly predictive for AKI [45]. The key inflammatory metabolite of tryptophan degradation, kynurenic acid, was significantly increased and associated with clinical outcomes in ICU patients with AKI [46,47]. In ischemia–reperfusion, cisplatin and sepsis-induced AKI animal models, there was a remarkably disturbed tryptophan metabolism and the metabolites catabolized by KP abnormally accumulated in kidney, urine or plasma [28,29,49]. The results in our present study were consistent with the previous studies, displaying a metabolic imbalance in tryptophan, while DMXAA significantly reduced the levels of kynurenine metabolites and upregulated tryptophan content in AKI mice, which reflected its regulatory effect on the tryptophan metabolism. Therefore, we speculate that the renoprotective of DMXAA functions through reversing the disturbance of tryptophan metabolism to some degree. Of course, extensive further studies are needed to clarify the exact role of tryptophan and its metabolites and their relationship between kynurenine metabolites and DMXAA.

DMXAA is an agonist of murine STING according to many references including the binding experiments [50–54]. In our study, we found that STING expression was significantly reduced by DMXAA in cisplatin-challenged wild-type mice. This phenomenon was consistent with the previous studies that STING agonist, such as dsDNA, HSV and DMXAA could trigger STING activation and induce its degradation [12,55,56]. The degradation of STING could serve as a negative regulation for STING signal pathway [55,56]. In agreement with this notion, our results showed that DMXAA could activate STING signaling along with the induction of STING degradation. However, the protective role of DMXAA was still observed in STING-deficient mice, which suggested that DMXAA could protect against cisplatin-induced AKI in a STING-independent manner in the present experimental setting. We speculated that DMXAA might have some other targets besides STING.

Some limitation of our study should be noted. First, we did not detect the role of DMXAA in other kinds of AKI mice models, which would expand the clinical application of DMXAA in the future. In addition, further studies are needed to clarify the exact role of DMXAA in metabolism, especially in tryptophan metabolism. On the other hand, there was a rising trend in AST level, which indicating a potential in liver injury following DMXAA treatment. Therefore, a special attention is suggested to be paid for liver function once DMXAA is used for treating diseases in clinic.

In summary, our study revealed a renoprotective role of DMXAA in cisplatin-induced AKI, including improved renal function and amelioration of renal tubular injury, cell apoptosis and inflammation. And this protective role of DMXAA was performed in a STING-independent manner. In fact, previous studies indicated that DMXAA enhanced the tumor cell killing of cisplatin, and co-administration of DMXAA produced a large enhancement of tumor growth delay with most of the cytotoxic drugs [57,58]. As our findings suggested that DMXAA can reduce cisplatin-induced nephrotoxicity, it is reasonable that the combination of DMXAA and cisplatin is a potential therapeutic strategy to combat certain cancers and cisplatin-induced AKI.

Clinical perspectives

- Although DMXAA is unable to bind human STING, it is still a prospective tumor-vascular disrupting agent and displays high efficiency for combination therapy with a wide spectrum of antitumor agents, including cisplatin.
- DMXAA markedly alleviated acute kidney injury induced by cisplatin possibly via suppressing inflammation and improving metabolic disorders, especially the tryptophan metabolism.
- Combination of DMXAA and cisplatin may be a potential therapeutic strategy to combat certain cancers and cisplatin-induced nephrotoxicity.

Data Availability

Raw data of RNA sequencing have been submitted to the public functional genomics data repository Gene Expression Omnibus (GEO, NO. GSE216295) and can be viewed at <https://www.ncbi.nlm.nih.gov/geo/query/acc.cgi?acc=GSE216295> by entering the secure token number: knivgmuwdjyzful. Raw data of metabolomics study has been deposited on the metabolomics database Metabolomics Workbench and can be temporarily available at <http://dev.metabolomicsworkbench.org:22222/data/DRCCMetadata.php?Mode=Study&StudyID=ST002390&Access=GpuQ2372> before being released on 2023-12-06.

Competing Interests

The authors declare that there are no competing interests associated with the manuscript.

Funding

This work was supported by grants from National Natural Science Foundation of China [grant numbers 81970581, 82170689, and 81873599]; the Nanjing Medical Science and Technique Development Foundation [grant numbers JQX21008 and JQX18007]; and the Postgraduate Research & Practice Innovation Program of Jiangsu Province [grant number KYCX21_1563].

CRedit Author Contribution

Lingling Lu: Visualization, Writing—original draft, Writing—review & editing. **Weihua Liu:** Validation, Investigation, Methodology. **Shumin Li:** Validation, Investigation, Methodology. **Mi Bai:** Funding acquisition, Investigation, Methodology. **Yu Zhou:** Validation, Investigation, Methodology. **Zhaohui Jiang:** Validation, Investigation, Methodology. **Zhanjun Jia:** Conceptualization, Data curation, Funding acquisition, Writing—review & editing. **Songming Huang:** Conceptualization, Data curation, Writing—review & editing. **Aihua Zhang:** Supervision, Project administration, Writing—review & editing. **Wei Gong:** Conceptualization, Funding acquisition, Investigation, Visualization, Methodology, Writing—original draft, Writing—review & editing.

Acknowledgements

The authors would like to thank Dr Xuan.zhou (Shanghai Luming Biotech. Co. Ltd) for assistance with the bioinformatics analysis.

Abbreviations

AHRR, aryl hydrocarbon receptor repressor; AKI, acute kidney injury; AST, aspartate aminotransferase; BUN, blood urea nitrogen; CK-MB, creatine kinase-MB; DEG, differentially expressed gene; ESI, electrospray ionization; FC, fold change; FDR, false discovery rate; GEO, Gene Expression Omnibus database; H&E, hematoxylin and eosin; KEGG, Kyoto Encyclopedia of Genes and Genomes; KIM-1, kidney injury molecule 1; KO, knockout; KP, kynurenine pathway; KYNA, kynurenic acid; LDH, lactate

dehydrogenase; MMP7, matrix metalloproteinase-7; NGAL, neutrophil gelatinase-associated lipocalin; PCA, principal component analysis; QC, quality control; qRT-PCR, quantitative real-time PCR; SAA, serum amyloid A protein; Scr, serum creatinine; STING, stimulator of interferon genes.

References

- Zhang, C., Xu, C., Gao, X. and Yao, Q. (2022) Platinum-based drugs for cancer therapy and anti-tumor strategies. *Theranostics* **12**, 2115–2132, <https://doi.org/10.7150/thno.69424>
- Oun, R., Moussa, Y.E. and Wheate, N.J. (2018) The side effects of platinum-based chemotherapy drugs: a review for chemists. *Dalton Trans.* **47**, 6645–6653, <https://doi.org/10.1039/C8DT00838H>
- Miller, R.P., Tadagavadi, R.K., Ramesh, G. and Reeves, W.B. (2010) Mechanisms of cisplatin nephrotoxicity. *Toxins (Basel)* **2**, 2490–2518, <https://doi.org/10.3390/toxins2112490>
- McSweeney, K.R., Gadanec, L.K., Qaradakh, T., Ali, B.A., Zulli, A. and Apostolopoulos, V. (2021) Mechanisms of Cisplatin-induced acute kidney injury: pathological mechanisms, pharmacological interventions, and genetic mitigations. *Cancers (Basel)* **13**, 1572, <https://doi.org/10.3390/cancers13071572>
- (2012) Section 2: AKI definition. *Kidney Int. Suppl.* **2**, 19–36, <https://doi.org/10.1038/kisup.2011.32>
- Gobbi, S., Belluti, F., Rampa, A. and Bisi, A. (2021) Flavonoid-inspired vascular disrupting agents: exploring flavone-8-acetic acid and derivatives in the new century. *Molecules* **26**, 4228, <https://doi.org/10.3390/molecules26144228>
- Daei Farshchi Adli, A., Jahanban-Esfahlan, R., Seidi, K., Samandari-Rad, S. and Zarghami, N. (2018) An overview on Vadimezan (DMXAA): The vascular disrupting agent. *Chem. Biol. Drug Des.* **91**, 996–1006, <https://doi.org/10.1111/cbdd.13166>
- Prantner, D., Perkins, D.J., Lai, W., Williams, M.S., Sharma, S., Fitzgerald, K.A. et al. (2012) 5,6-Dimethylxanthone-4-acetic acid (DMXAA) activates stimulator of interferon gene (STING)-dependent innate immune pathways and is regulated by mitochondrial membrane potential. *J. Biol. Chem.* **287**, 39776–39788, <https://doi.org/10.1074/jbc.M112.382986>
- McKeage, M.J. and Baguley, B.C. (2010) Disrupting established tumor blood vessels: an emerging therapeutic strategy for cancer. *Cancer* **116**, 1859–1871, <https://doi.org/10.1002/cncr.24975>
- Ding, C., Song, Z., Shen, A., Chen, T. and Zhang, A. (2020) Small molecules targeting the innate immune cGAS/STING/TBK1 signaling pathway. *Acta Pharm. Sin. B.* **10**, 2272–2298, <https://doi.org/10.1016/j.apsb.2020.03.001>
- Kim, S., Li, L., Maliga, Z., Yin, Q., Wu, H. and Mitchison, T.J. (2013) Anticancer flavonoids are mouse-selective STING agonists. *ACS Chem. Biol.* **8**, 1396–1401, <https://doi.org/10.1021/cb400264n>
- Corrales, L., Glickman, L.H., McWhirter, S.M., Kanne, D.B., Sivick, K.E., Katibah, G.E. et al. (2015) Direct activation of STING in the Tumor microenvironment leads to potent and systemic tumor regression and immunity. *Cell Rep.* **11**, 1018–1030, <https://doi.org/10.1016/j.celrep.2015.04.031>
- Maekawa, H., Inoue, T., Ouchi, H., Jao, T.M., Inoue, R., Nishi, H. et al. (2019) Mitochondrial damage causes inflammation via cGAS-STING signaling in acute kidney injury. *Cell Rep.* **29**, 1261e6–1273e6, <https://doi.org/10.1016/j.celrep.2019.09.050>
- Gong, W., Lu, L., Zhou, Y., Liu, J., Ma, H., Fu, L. et al. (2021) The novel STING antagonist H151 ameliorates cisplatin-induced acute kidney injury and mitochondrial dysfunction. *Am. J. Physiol. Renal. Physiol.* **320**, F608–F616, <https://doi.org/10.1152/ajprenal.00554.2020>
- Chin, E.N., Yu, C., Vartabedian, V.F., Jia, Y., Kumar, M., Gamo, A.M. et al. (2020) Antitumor activity of a systemic STING-activating non-nucleotide cGAMP mimetic. *Science* **369**, 993–999, <https://doi.org/10.1126/science.abb4255>
- Weidemann, A., Bernhardt, W.M., Klanke, B., Daniel, C., Buchholz, B., Campean, V. et al. (2008) HIF activation protects from acute kidney injury. *J. Am. Soc. Nephrol.* **19**, 486–494, <https://doi.org/10.1681/ASN.2007040419>
- Yang, Y., Yu, X., Zhang, Y., Ding, G., Zhu, C., Huang, S. et al. (2018) Hypoxia-inducible factor prolyl hydroxylase inhibitor roxadustat (FG-4592) protects against cisplatin-induced acute kidney injury. *Clin. Sci. (Lond.)* **132**, 825–838, <https://doi.org/10.1042/CS20171625>
- Kim, J.Y., Bai, Y., Jayne, L.A., Abdulkader, F., Gandhi, M., Perreau, T. et al. (2020) SOX9 promotes stress-responsive transcription of VGF nerve growth factor inducible gene in renal tubular epithelial cells. *J. Biol. Chem.* **295**, 16328–16341, <https://doi.org/10.1074/jbc.RA120.015110>
- Bai, M., Chen, H., Ding, D., Song, R., Lin, J., Zhang, Y. et al. (2019) MicroRNA-214 promotes chronic kidney disease by disrupting mitochondrial oxidative phosphorylation. *Kidney Int.* **95**, 1389–1404, <https://doi.org/10.1016/j.kint.2018.12.028>
- Nakayama, K., Saito, S., Watanabe, K., Miyashita, H., Nishijima, F., Kamo, Y. et al. (2017) Influence of AHRP Pro189Ala polymorphism on kidney functions. *Biosci. Biotechnol. Biochem.* **81**, 1120–1124, <https://doi.org/10.1080/09168451.2017.1292838>
- Hsu, S.H., Chou, L.F., Hong, C.H., Chang, M.Y., Tsai, C.Y., Tian, Y.C. et al. (2021) Crosstalk between E-Cadherin/beta-Catenin and NF-kappaB Signaling Pathways: The Regulation of Host-Pathogen Interaction during Leptospirosis. *Int. J. Mol. Sci.* **22**, 13132, <https://doi.org/10.3390/ijms222313132>
- Kelly, K.J., Kluge-Beckerman, B., Zhang, J. and Dominguez, J.H. (2010) Intravenous cell therapy for acute renal failure with serum amyloid A protein-reprogrammed cells. *Am. J. Physiol. Renal. Physiol.* **299**, F453–F464, <https://doi.org/10.1152/ajprenal.00050.2010>
- Piedrafitra, A., Balayssac, S., Casemayou, A., Saulnier-Blache, J.S., Lucas, A., Iacovoni, J.S. et al. (2021) Hepatocyte nuclear factor-1beta shapes the energetic homeostasis of kidney tubule cells. *FASEB J.* **35**, e21931, <https://doi.org/10.1096/fj.202100782RR>
- Naito, Y., Tsuji, T., Nagata, S., Tsuji, N., Fujikura, T., Ohashi, N. et al. (2020) IL-17A activated by Toll-like receptor 9 contributes to the development of septic acute kidney injury. *Am. J. Physiol. Renal. Physiol.* **318**, F238–F247, <https://doi.org/10.1152/ajprenal.00313.2019>
- Cervenka, I., Agudelo, L.Z. and Ruas, J.L. (2017) Kynurenines: Tryptophan's metabolites in exercise, inflammation, and mental health. *Science* **357**, <https://doi.org/10.1126/science.aaf9794>
- Platten, M., Nollen, E.A.A., Rohrig, U.F., Fallarino, F. and Opitz, C.A. (2019) Tryptophan metabolism as a common therapeutic target in cancer, neurodegeneration and beyond. *Nat. Rev. Drug Discov.* **18**, 379–401, <https://doi.org/10.1038/s41573-019-0016-5>

- 27 Davidson, J.A., Robison, J., Khailova, L., Frank, B.S., Jaggars, J., Ing, R.J. et al. (2022) Metabolomic profiling demonstrates evidence for kidney and urine metabolic dysregulation in a piglet model of cardiac surgery-induced acute kidney injury. *Am. J. Physiol. Renal. Physiol.* **323**, F20–F32, <https://doi.org/10.1152/ajprenal.00039.2022>
- 28 Dai, M., Wang, Q., Kou, S., Li, X., Jiang, Z., Sun, L. et al. (2022) A sensitive UPLC-MS/MS method for the simultaneous determination of the metabolites in the tryptophan pathway in rat plasma. *J. Pharm. Biomed. Anal.* **219**, 114979, <https://doi.org/10.1016/j.jpba.2022.114979>
- 29 Tan, B., Chen, J., Qin, S., Liao, C., Zhang, Y., Wang, D. et al. (2021) Tryptophan pathway-targeted metabolomics study on the mechanism and intervention of cisplatin-induced acute kidney injury in rats. *Chem. Res. Toxicol.* **34**, 1759–1768, <https://doi.org/10.1021/acs.chemrestox.1c00110>
- 30 Ching, L.M., Zwain, S. and Baguley, B.C. (2004) Relationship between tumour endothelial cell apoptosis and tumour blood flow shutdown following treatment with the antivasular agent DMXAA in mice. *Br. J. Cancer* **90**, 906–910, <https://doi.org/10.1038/sj.bjc.6601606>
- 31 Przespolewski, A.C., Portwood, S. and Wang, E.S. (2022) Targeting acute myeloid leukemia through multimodal immunotherapeutic approaches. *Leuk. Lymphoma* **63** (4), 918–927, <https://doi.org/10.1080/10428194.2021.199261>
- 32 Yu, Y., Liu, Y., An, W., Song, J., Zhang, Y. and Zhao, X. (2019) STING-mediated inflammation in Kupffer cells contributes to progression of nonalcoholic steatohepatitis. *J. Clin. Invest.* **129**, 546–555, <https://doi.org/10.1172/JCI121842>
- 33 Baguley, B.C. and Ching, L.M. (2002) DMXAA: an antivasular agent with multiple host responses. *Int. J. Radiat. Oncol. Biol. Phys.* **54**, 1503–1511, [https://doi.org/10.1016/S0360-3016\(02\)03920-2](https://doi.org/10.1016/S0360-3016(02)03920-2)
- 34 Zwi, L.J., Baguley, B.C., Gavin, J.B. and Wilson, W.R. (1994) The morphological effects of the anti-tumor agents flavone acetic acid and 5,6-dimethyl xanthone acetic acid on the colon 38 mouse tumor. *Pathology* **26**, 161–169
- 35 Hu, Q., Ren, H., Li, G., Wang, D., Zhou, Q., Wu, J. et al. (2019) STING-mediated intestinal barrier dysfunction contributes to lethal sepsis. *EBioMedicine* **41**, 497–508, <https://doi.org/10.1016/j.ebiom.2019.02.055>
- 36 Wang, M., Lee, E., Song, W., Ricciotti, E., Rader, D.J., Lawson, J.A. et al. (2008) Microsomal prostaglandin E synthase-1 deletion suppresses oxidative stress and angiotensin II-induced abdominal aortic aneurysm formation. *Circulation* **117**, 1302–1309, <https://doi.org/10.1161/CIRCULATIONAHA.107.731398>
- 37 Jia, Z., Guo, X., Zhang, H., Wang, M.H., Dong, Z. and Yang, T. (2008) Microsomal prostaglandin synthase-1-derived prostaglandin E2 protects against angiotensin II-induced hypertension via inhibition of oxidative stress. *Hypertension* **52**, 952–959, <https://doi.org/10.1161/HYPERTENSIONAHA.108.111229>
- 38 Cao, L., Xu, E., Zheng, R., Zhangchen, Z., Zhong, R., Huang, F. et al. (2022) Traditional Chinese medicine Lingguizhugan decoction ameliorate HFD-induced hepatic-lipid deposition in mice by inhibiting STING-mediated inflammation in macrophages. *Chin. Med.* **17**, 7, <https://doi.org/10.1186/s13020-021-00559-3>
- 39 Wei, Q., Xiao, X., Fogle, P. and Dong, Z. (2014) Changes in metabolic profiles during acute kidney injury and recovery following ischemia/reperfusion. *PLoS ONE* **9**, e106647, <https://doi.org/10.1371/journal.pone.0106647>
- 40 Irie, M., Hayakawa, E., Fujimura, Y., Honda, Y., Setoyama, D., Wariishi, H. et al. (2018) Analysis of spatiotemporal metabolomic dynamics for sensitively monitoring biological alterations in cisplatin-induced acute kidney injury. *Biochem. Biophys. Res. Commun.* **496**, 140–146, <https://doi.org/10.1016/j.bbrc.2018.01.012>
- 41 Chihanga, T., Ruby, H.N., Ma, Q., Bashir, S., Devarajan, P. and Kennedy, M.A. (2018) NMR-based urine metabolic profiling and immunohistochemistry analysis of nephron changes in a mouse model of hypoxia-induced acute kidney injury. *Am. J. Physiol. Renal. Physiol.* **315**, F1159–F1173, <https://doi.org/10.1152/ajprenal.00500.2017>
- 42 Piret, S.E. and Mallipattu, S.K. (2022) Transcriptional regulation of proximal tubular metabolism in acute kidney injury. *Pediatr. Nephrol.* **38** (4), 975–986, <https://doi.org/10.1007/s00467-022-05748-2>
- 43 Jenkins, T.A., Nguyen, J.C., Polglaze, K.E. and Bertrand, P.P. (2016) Influence of tryptophan and serotonin on mood and cognition with a possible role of the gut-brain axis. *Nutrients* **8**, 56, <https://doi.org/10.3390/nu8010056>
- 44 Guillemin, G.J., Cullen, K.M., Lim, C.K., Smythe, G.A., Garner, B., Kapoor, V. et al. (2007) Characterization of the kynurenine pathway in human neurons. *J. Neurosci.* **27**, 12884–12892, <https://doi.org/10.1523/JNEUROSCI.4101-07.2007>
- 45 Nadour, Z., Simian, C., Laprevote, O., Lorient, M.A., Larabi, I.A. and Pallet, N. (2022) Validation of a liquid chromatography coupled to tandem mass spectrometry method for simultaneous quantification of tryptophan and 10 key metabolites of the kynurenine pathway in plasma and urine: Application to a cohort of acute kidney injury patients. *Clin. Chim. Acta* **534**, 115–127, <https://doi.org/10.1016/j.cca.2022.07.009>
- 46 Aregger, F., Uehlinger, D.E., Fusch, G., Bahonjic, A., Pschowski, R., Walter, M. et al. (2018) Increased urinary excretion of kynurenic acid is associated with non-recovery from acute kidney injury in critically ill patients. *BMC Nephrol.* **19**, 44, <https://doi.org/10.1186/s12882-018-0841-5>
- 47 Dabrowski, W., Kocki, T., Pilat, J., Parada-Turska, J. and Malbrain, M.L. (2014) Changes in plasma kynurenic acid concentration in septic shock patients undergoing continuous veno-venous haemofiltration. *Inflammation* **37**, 223–234, <https://doi.org/10.1007/s10753-013-9733-9>
- 48 Zakrocka, I. and Zaluska, W. (2022) Kynurenine pathway in kidney diseases. *Pharmacol. Rep.* **74**, 27–39, <https://doi.org/10.1007/s43440-021-00329-w>
- 49 Qu, X., Gao, H., Sun, J., Tao, L., Zhang, Y., Zhai, J. et al. (2020) Identification of key metabolites during cisplatin-induced acute kidney injury using an HPLC-TOF/MS-based non-targeted urine and kidney metabolomics approach in rats. *Toxicology* **431**, 152366, <https://doi.org/10.1016/j.tox.2020.152366>
- 50 Conlon, J., Burdette, D.L., Sharma, S., Bhat, N., Thompson, M., Jiang, Z. et al. (2013) Mouse, but not human STING, binds and signals in response to the vascular disrupting agent 5,6-dimethylxanthone-4-acetic acid. *J. Immunol.* **190**, 5216–5225, <https://doi.org/10.4049/jimmunol.1300097>
- 51 Deng, L., Liang, H., Xu, M., Yang, X., Burnette, B., Arina, A. et al. (2014) STING-dependent cytosolic DNA sensing promotes radiation-induced type I interferon-dependent antitumor immunity in immunogenic tumors. *Immunity* **41**, 843–852, <https://doi.org/10.1016/j.immuni.2014.10.019>
- 52 Gao, P., Ascano, M., Zillinger, T., Wang, W., Dai, P., Serganov, A.A. et al. (2013) Structure-function analysis of STING activation by c[G(2',5')pA(3',5')p] and targeting by antiviral DMXAA. *Cell* **154**, 748–762, <https://doi.org/10.1016/j.cell.2013.07.023>

- 53 Gao, P., Zillinger, T., Wang, W., Ascano, M., Dai, P., Hartmann, G. et al. (2014) Binding-pocket and lid-region substitutions render human STING sensitive to the species-specific drug DMXAA. *Cell Rep.* **8**, 1668–1676, <https://doi.org/10.1016/j.celrep.2014.08.010>
- 54 Lou, Y.C., Kao, Y.F., Chin, K.H., Chen, J.K., Tu, J.L., Chen, C. et al. (2015) Backbone resonance assignments of the 54 kDa dimeric C-terminal domain of murine STING in complex with DMXAA. *Biomol. NMR Assign* **9**, 271–274, <https://doi.org/10.1007/s12104-014-9590-y>
- 55 Gonugunta, V.K., Sakai, T., Pokatayev, V., Yang, K., Wu, J., Dobbs, N. et al. (2017) Trafficking-mediated STING degradation requires sorting to acidified endolysosomes and can be targeted to enhance anti-tumor response. *Cell Rep.* **21**, 3234–3242, <https://doi.org/10.1016/j.celrep.2017.11.061>
- 56 Hu, Y., Li, X., Wang, D. and Mao, X. (2023) mascRNA alleviates STING-TBK1 signaling-mediated immune response through promoting ubiquitination of STING. *Mol. Immunol.* **154**, 45–53, <https://doi.org/10.1016/j.molimm.2022.12.012>
- 57 Siim, B.G., Lee, A.E., Shalal-Zwain, S., Pruijn, F.B., McKeage, M.J. and Wilson, W.R. (2003) Marked potentiation of the antitumour activity of chemotherapeutic drugs by the antivascular agent 5,6-dimethylxanthenone-4-acetic acid (DMXAA). *Cancer Chemother. Pharmacol.* **51**, 43–52, <https://doi.org/10.1007/s00280-002-0529-0>
- 58 Siemann, D.W., Mercer, E., Lepler, S. and Rojiani, A.M. (2002) Vascular targeting agents enhance chemotherapeutic agent activities in solid tumor therapy. *Int. J. Cancer* **99**, 1–6, <https://doi.org/10.1002/ijc.10316>
- 59 Lingling, L., Shumin, L., Weihua, L., Songming, H., Aihua, Z. and Wei, G. (2022) Gene expression profiling of renal tissues isolated from C57BL/6J mice treated with DMXAA: Gene Expression Omnibus. [updated 2022.10. Available from: <https://www.ncbi.nlm.nih.gov/geo/query/acc.cgi?acc=GSE216295>
- 60 Lingling, L. (2022) The metabolomic resetting effect of DMXAA in cisplatin-induced AKI: Metabolights. [updated 2022.12. Available from: <http://dev.metabolomicsworkbench.org:22222/data/DRCCMetadata.php?Mode=Study&StudyID=ST002390&Access=GpuQ2372>